Int. J. Electrochem. Sci., 13 **(2018)** 5054 – 5060, doi: 10.20964/2018.05.86

International Journal of
ELECTROCHEMICAL
SCIENCE
www.electrochemsci.org

Short Communication

Intermediate Temperature Electrochemical Properties of Yb^{3+} Doped $SrCeO_3$- carbonate and Chloride Composite Electrolytes

Lin Sun, Ruifeng Du, Hongtao Wang[*], *Huiquan Li*[**]

School of Chemical and Material Engineering, Fuyang Normal College; Anhui Provincial Key Laboratory for Degradation and Monitoring of Pollution of the Environment, Fuyang 236037, China
[*]E-mail: hongtaoking3@163.com, huiquanli0908@163.com

Received: 4 December 2017 / *Accepted:* 18 January 2018 / *Published:* 10 April 2018

In this work, novel $SrCe_{0.9}Yb_{0.1}O_{3-\alpha}$-$(Li/Na)_2CO_3$ (SCYb-LN) and $SrCe_{0.9}Yb_{0.1}O_{3-\alpha}$-LiCl-$SrCl_2$ (SCYb-LS) electrolyte composites were successfully fabricated at low temperature. The SEM image results show that the composites possess sufficient density. The highest conductivity is observed to be 3.5×10^{-2} and 1.2×10^{-1} $S\cdot cm^{-1}$ for SCYb-LS, SCYb-LN at 600 °C, respectively. In a hydrogen-containing atmosphere, the composites are almost pure ionic conductors, according to the log $\sigma \sim$ log (pO_2) plots results. Using SCYb-LN and SCYb-LS as electrolytes, the H_2/O_2 fuel cells produce the maximum power densities of 294 and 147 $mW\cdot cm^{-2}$ at 600 °C, correspondingly.

Keywords: $SrCeO_3$; Composite; Electrolyte; Fuel cell; Conductivity

1. INTRODUCTION

Recently, electrolytes possessing high conductivities at 400–800 °C have been successfully developed in intermediate temperature fuel cells (ITFCs) [1–2]. In recent decades, carbonate composites doped with cerium oxide have been extensively investigated [3–7]. For example, using a citrate-based route, Marques et al. prepared $Ce_{0.9}Eu_{0.1}O_{2-\alpha}$-$(Li,Na)_2CO_3$ composites [3]. Huang et al. studied the conductivity and fuel cell performance of $BaCe_{0.7}Zr_{0.1}Y_{0.2}O_{3-\alpha}$-$(Li,Na)_2CO_3$ composites [4]. Park et al. reported on $Ce_{0.8}Nd_{0.2}O_{2-\alpha}$-$(Li,Na)_2CO_3$ composite electrolytes and studied the multi-ionic conduction at intermediate temperatures [5].

High temperature proton conductors (HTPCs) are utilized in numerous electrochemical processes, such as hydrogen production, hydrogen sensors and solid oxide fuel cells (SOFCs) etc. [8–10]. In recent decades, perovskite-type oxide has become considered a promising candidate material for reducing SOFCs working temperature from 400 °C to 800 °C. The proton conductivity in a

hydrogen-containing atmosphere of strontium-cerium type perovskite(ABO_3) materials has been previously reported [11–20]. Fu et al. reported on K^+ and Y^{3+} substituted for Sr^{2+} and Ce^{4+} in $SrCeO_3$ and studied the conductivity and chemical stability [12]. Li et al. synthesized $SrCe_{0.9}Yb_{0.1}O_{3-\alpha}$ at low temperature by a gel combustion method [16]. Usually, Yb and Y doped $SrCeO_3$ have the best performance. Therefore, ytterbium was selected to partially replace the site of B atom for $SrCeO_3$ in this work. In our previous study, we explored the influence of three different inorganic salts and the results indicated that the intermediate temperature electrochemical properties of $SrCe_{0.9}Yb_{0.1}O_{3-\alpha}$-NaCl-KCl were higher than those of $SrCe_{0.9}Yb_{0.1}O_{3-\alpha}$-$Li_2CO_3$-$K_2CO_3$ and $SrCe_{0.9}Yb_{0.1}O_{3-\alpha}$-NaCl-$CaCl_2$ [21].

In this work, we prepared two other different types of inorganic salts-$SrCe_{0.9}Yb_{0.1}O_{3-\alpha}$ composite electrolytes, $SrCe_{0.9}Yb_{0.1}O_{3-\alpha}$-$(Li/Na)_2CO_3$ (SCYb-LN) and $SrCe_{0.9}Yb_{0.1}O_{3-\alpha}$-LiCl-$SrCl_2$ (SCYb-LS), in order to find the inorganic salt with the best performance. The conduction behaviors from 400 °C to 600 °C were investigated using electrochemical methods. Using the composite as electrolytes, the properties of H_2/O_2 fuel cells were also tested.

2. EXPERIMENT

$SrCe_{0.9}Yb_{0.1}O_{3-\alpha}$ was fabricated according to previous reports [11,12,14,15,18]. First, weighed powders of CeO_2, Yb_2O_3 and $SrCO_3$ were of analytical-grade and were heated to 1300 °C (5 h). The synthetic sample was ground, calcined at 1500 °C (5 h) in air, and marked as SCYb.

The mole ratio of Li_2CO_3/Na_2CO_3 was controlled at 1:1[22], but the mole ratio of LiCl/$SrCl_2$ was controlled at 1.7:1. Then, the molten salt was obtained by the solid mixtures which were calcined at 580 °C (2 h). 80 wt% SCYb powder was mixed with 20 wt% Li_2CO_3/Na_2CO_3 and LiCl/$SrCl_2$. The mixtures were ground, sieved (100 mesh) and pressed into pellet under 200 MPa pressure. Finally, the $SrCe_{0.9}Yb_{0.1}O_{3-\alpha}$-$(Li/Na)_2CO_3$ (SCYb-LN) and $SrCe_{0.9}Yb_{0.1}O_{3-\alpha}$-LiCl-$SrCl_2$ (SCYb-LS) electrolytes were obtained by the above mixtures being calcined at 600 °C (1 h).

Using X–ray powder diffraction (XRD), the crystalline structure of the SCYb-LN and SCYb-LS electrolytes were determined at room temperature. Scanning electron microscope (SEM) was used to study the microstructure of the electrolytes.

In order to determine the electrochemical properties, round plates of ~18 mm in diameter and 1.0–1.2 mm thickness were fabricated. 20%Pd-80%Ag paste was smeared on both sides (0.5 cm^2) of the round plates, and used as electrodes. The impedance spectra were investigated by using a CHI660E electrochemical analyzer from 1 Hz to 1 MHz. In dry N_2, the conductivity measurements as a temperature function were also studied. Dry experimental atmospheres were acquired by using P_2O_5.In the pO_2 range of $1–10^{-20}$ atm, the conductivity as the function of oxygen partial pressure (pO_2) was measured. The pO_2 was achieved by commixing O_2, air, N_2 and H_2 in a proper ratio and measured by using an oxygen sensor. Finally, the H_2/O_2 fuel cells were fabricated.

3. RESULTS AND DISCUSSION

The X–ray diffraction (XRD) patterns of SCYb-LN and SCYb-LS are shown in Fig. 1. It can be seen from Fig. 1 that diffractions for $SrCeO_3$ phase in JCPDS (01-082-2370) are found in the as-

prepared composite electrolytes. At the same time, some NaCl and $SrCl_2$ peaks are also observed. However, the much lower intensity of these reflections suggests that carbonate or chloride crystallites are less developed. As amorphous salt, most of them are in the grain boundary of $SrCe_{0.9}Yb_{0.1}O_{3-\alpha}$ crystal. This has been proven by other research [3,23-25]. Marques et al. reported that there is no reaction between Gd-doped ceria and $(Li,Na)_2CO_3$ carbonates [23].

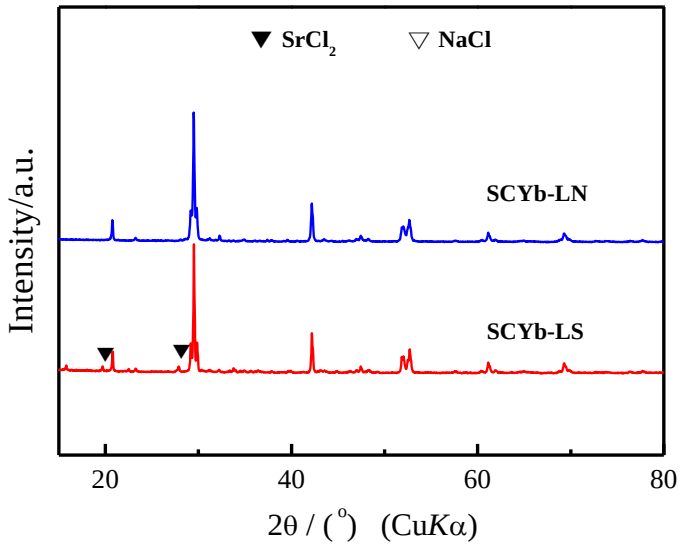

Figure 1. XRD patterns of the SCYb-LN and SCYb-LS.

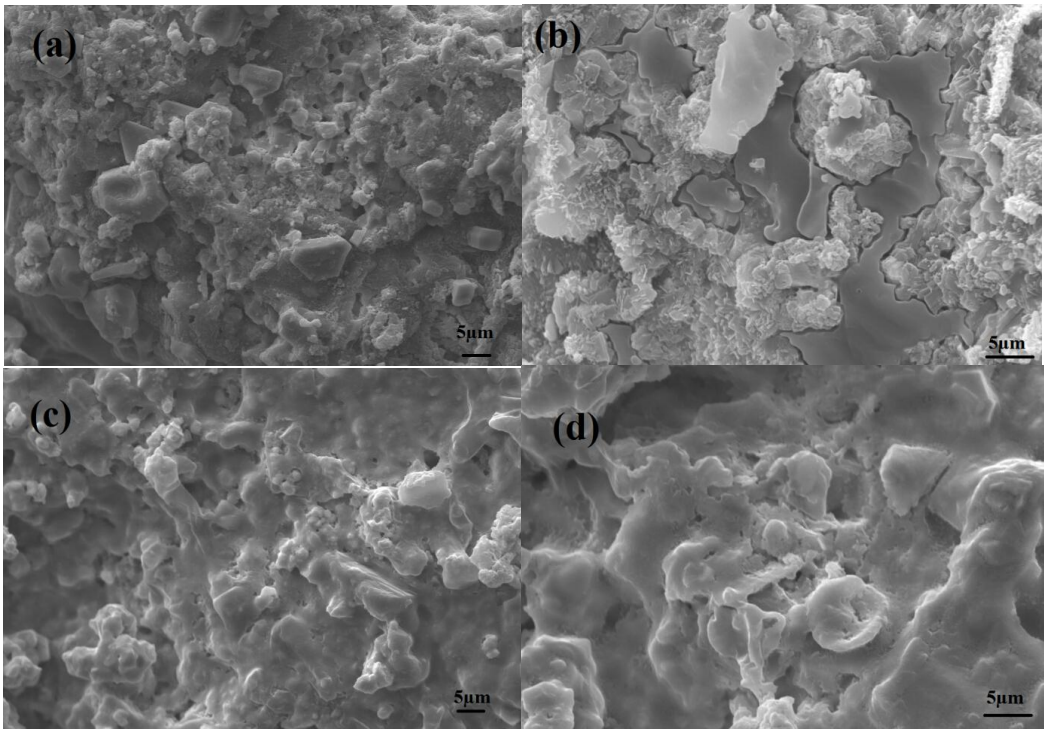

Figure 2. (a-d) The cross-sectional and external surface SEM images of SCYb-LN and SCYb-LS.

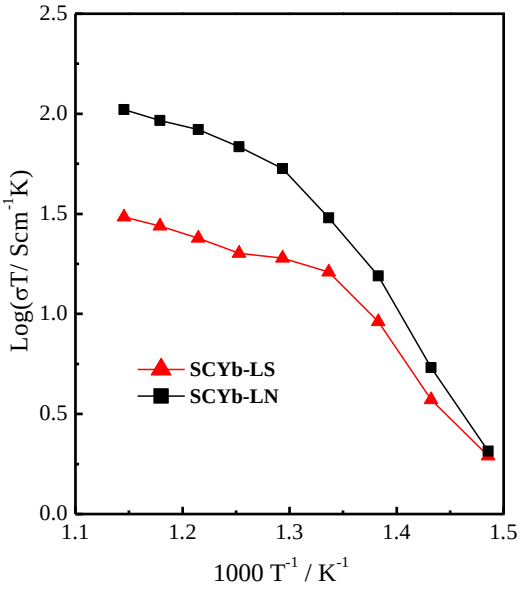

Figure 3. Temperature dependence of conductivities of the SCYb-LS and SCYb-LN in dry N_2 atmosphere from 400 °C to 600 °C.

Fig. 2 displays the SEM images of cross-sectional and external surface of the above composites. In Fig. 2, it can be seen that the composites are especially dense and the molten LiCl/$SrCl_2$ and Li_2CO_3/Na_2CO_3 covered the $SrCe_{0.9}Yb_{0.1}O_{3-\alpha}$ particle surfaces uniformly. The molten carbonate and chloride appear to be used as the glue of $SrCe_{0.9}Yb_{0.1}O_{3-\alpha}$ particles, which is similar to the result of ceria-carbonates composites fabricated via similar calcine treatments [26–28]. Meng et al. reported gadolinium-dopedceria(GDC)-LiCl-$SrCl_2$ was fully densified and no pore were observed [27–28].

In a dry N_2 atmosphere, the Arrhenius plots of conductivity for SCYb-LS and SCYb-LN from 400 °C to 600 °C are shown in Fig. 3. As can be seen from Fig. 3, a sharp conductivity jump is seen around 500 °C and the conductivities are between 0.068 and 0.12 $S \cdot cm^{-1}$ for SCY-LN, between 0.024 and 0.035 $S \cdot cm^{-1}$ for SCY-LS in the 500–600 °C temperature range, respectively, which are higher than that of Yb and Y doped $SrCeO_3$ [12–16]. It is concluded that the conductivities are enhanced by the introduction of carbonate and chloride. The improved conductivity of the composites might be attributed to the carbonate and chloride molten phase and the interfaces between amorphous salt with another fast ionic transport way and $SrCe_{0.9}Yb_{0.1}O_{3-\alpha}$ particles [2–5].

To study the ionic conduction of the above three composites, Fig. 4 shows the dependence of conductivity for the partial pressure of oxygen (pO_2 = 10^{-20}～1 atm) in dry atmospheres. It can be observed in Fig. 4, in a hydrogen-containing atmosphere, there is obviously no variation of conductivity with pO_2. This implies that they are pure ion conductors. Under oxidizing conditions, it can also be seen from Fig. 4 that the conductivity decreases with increasing pO_2. At high oxygen partial pressure, it can be attributed to the fact that the electronic holes and oxide ions generated from the $SrCe_{0.9}Yb_{0.1}O_{3-\alpha}$composite cannot move easily through the molten inorganic salt eutectic[5].

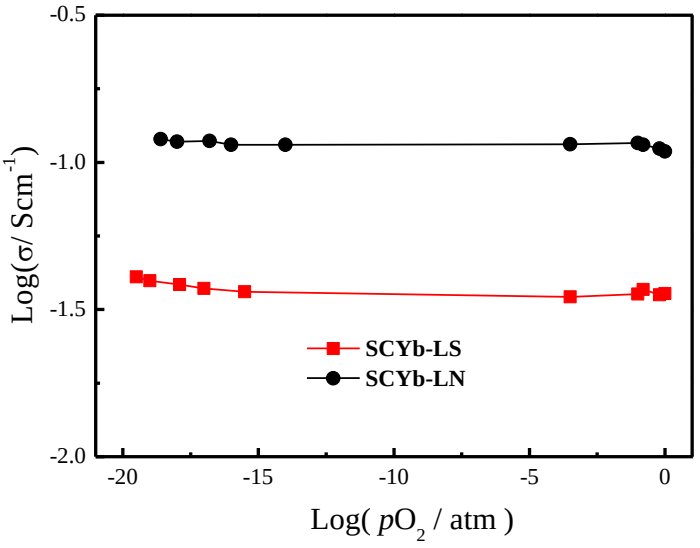

Figure 4. The conductivity of SCYb-LS and SCYb-LN as a function of pO_2.

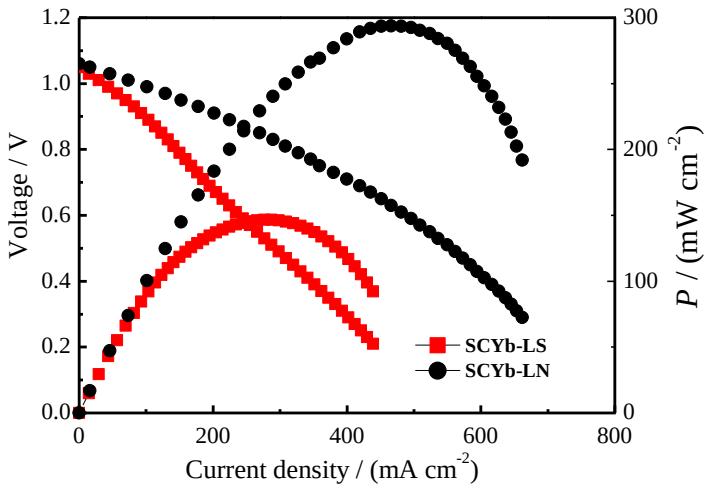

Figure 5. The *I-V* and *I-P* curves of H_2/O_2 fuel cells for the SCYb-LS and SCYb-LN at 600 °C.

Fig. 5 illustrates the *I-V* and *I-P* curves of the H_2/O_2 fuel cells for the SCYb-LS and SCYb-LN at 600 °C. It can be observed in Fig. 5 that the open circuit voltage is ~1.05 V. This shows that all the composites possess sufficient density. When temperature reaches the melting point (~500 °C), the molten carbonate and chloride will load the interspace of $SrCe_{0.9}Yb_{0.1}O_{3-\alpha}$ particles, forming relatively dense composite electrolytes.

According to the *I-P* characteristics, the best performances of SCY-LN is 294 $mW \cdot cm^{-2}$ power density output, corresponding to ~466 $mA \cdot cm^{-2}$ current density output at 600 °C. Based on the dense

SCY-LS composite, the fuel cell also shows good cell properties with maximum 147 $mW \cdot cm^{-2}$ power output densities at 600 °C, respectively.

4. CONCLUSIONS

In this work, $SrCe_{0.9}Yb_{0.1}O_{3-\alpha}$-$(Li/Na)_2CO_3$ (SCYb-LN) and $SrCe_{0.9}Yb_{0.1}O_{3-\alpha}$-LiCl-$SrCl_2$ (SCYb-LS) electrolytes were fabricated at low temperature. The XRD results show that most carbonate and chloride are used as amorphous salt in the $SrCe_{0.9}Yb_{0.1}O_{3-\alpha}$ crystal grain boundary. The SEM image results imply that the composites possess good density. The conductivity is between 0.068 and 0.12 $S \cdot cm^{-1}$ for SCYb-LN, between 0.024 and 0.035 $S \cdot cm^{-1}$ for SCYb-LS in the 500–600 °C temperature range, respectively. The best performances of SCYb-LN with the power density output of 294 $mW \cdot cm^{-2}$ corresponding to the current density output around 466 $mA \cdot cm^{-2}$ at 600 °C.

ACKNOWLEDGEMENTS
This study is supported by the National Natural Science Foundation of China (No. 51402052), Anhui Province Foundation (No. 1608085MB34, KJ2017ZD28), Scientific Research of Fuyang Normal College (2017FSKJ03ZD), Horizontal cooperation project of Fuyang municipal government and Fuyang Normal College (No. XDHX2016002, XDHX2016019).

References

1. S. Su, S. Zhang, C. Yan, Z. Yang, F. Zheng and L. Zhang, *Int. J. Electrochem. Sci.*, 12 (2017) 230.
2. L. Fang, *Int. J. Electrochem. Sci*., 12 (2017) 218.
3. S. Rajesh, D.A. Macedo, R.M. Nascimento, G.L. Souza, F.M.L. Figueiredo and F.M.B. Marques, *Int. J. Hydrogen Energ.*, 38 (2013) 16539.
4. Y. Hei, J. Huang, C. Wang and Z. Mao, *Int. J. Hydrogen Energ.*, 39 (2014) 14328.
5. J.T. Kim, T.H. Lee, K.Y. Park, Y. Seo, K.B. Kim, S.J. Song, B. Park and J.Y. Park, *J. Power Sources*, 275 (2015) 563.
6. J. Huang, Z. Mao, Z. Liu and C. Wang, *J. Power Sources*, 175 (2008) 238.
7. F. Xie, C. Wang, Z. Mao and Z. Zhan, *Int. J. Hydrogen Energ.*, 39 (2014) 14397.
8. C. Li, R. Dai, R. Qi, X. Wu and J. Ma, *Int. J. Electrochem. Sci*., 12 (2017) 2485.
9. D.-K. Lim, J.-H. Kim, A.U. Chavan, T.-R. Lee, Y.-S. Yoo and S.-J. Song, *Ceram. Int.*, 42 (2016) 3776.
10. Q. Hu, F. Yang, H. Fang and C. Zhao, *Int. J. Electrochem. Sci.*, 12 (2017) 7411.
11. K.-T. Hsu, J. S.-C. Jang, Y.-J. Ren, P.-H. Tsai, C. Li, C.-J. Tseng, J.-C. Lin, C.-S. Hsi and I-M. Hung, *J. Alloy Compd.*, 615 (2014) S491.
12. C. Liu, J.-J. Huang, Y.-P. Fu, C. Li, J.-Y. Wang and S. Lee, *Ceram. Int.*, 41 (2015) 2948.
13. I.-M. Hung, Y.-J. Chiang, J. S.-C. Jang, J.-C. Lin, S.-W. Lee, J.-K. Chang and C.-S. His, *J. Eur. Ceram. Soc.*, 35 (2015) 163.
14. N. Sammes, R. Phillips and A. Smirnova, *J. Power Sources*, 134 (2004) 153.
15. Y. Okuyama, K. Isa, Y.S. Lee, T. Sakai and H. Matsumoto, *Solid State Ionics*, 275 (2015) 35.
16. C. Zhang, S. Li, X. Liu, X. Zhao, D. He, H. Qiu, Q. Yu, S. Wang and L. Jiang, *Int. J. Hydrogen Energ.*, 38 (2013) 12921.

17. W. Xing, P.I. Dahl, L.V. Roaas, M.-L. Fontaine, Y. Larring, P.P. Henriksen and R. Bredesen, *J. Membrane Sci.*, 473(2015)327.
18. N.I. Matskevich, Th. Wolf, I.V. Vyazovkin and P. Adelmann, *J. Alloy Compd.*, 628 (2015) 126.
19. U.N. Shrivastava, K.L. Duncan and J.N. Chung, Int. *J. Hydrogen Energ.*, 37 (2012) 15350.
20. W. Yuan, C. Xiao and L. Li, *J. Alloy Compd.*, 616 (2014) 142.
21. W. Zhang, M. Yuan, H. Wang and J. Liu, *J. Alloy Compd.*, 677 (2016) 38.
22. J. Huang, Z. Gao and Z. Mao, *Int. J. Hydrogen Energ.*, 35 (2010) 4270.
23. A.I.B. Rondao, S.G. Patricio, F.M.L. Figueiredo and F.M.B. Marques, *Int. J. Hydrogen Energ.*, 39 (2014) 5460.
24. S. Shawuti and M.A. Gulgun, *J. Power Sources*, 267 (2014) 128.
25. N.C.T. Martins, S. Rajesh and F.M.B. Marques, *Mater. Res. Bull.*, 70 (2015) 449.
26. B. Zhu, S. Li and B.E. Mellander, *Electrochem. Commun.*, 10 (2008) 302.
27. Q.X. Fu, W. Zhang, R.R. Peng, D.K. Peng, G.Y. Meng and B. Zhu, *Mater. Lett.*, 53 (2002) 186.
28. Q.X. Fu, S.W. Zha, W. Zhang, D.K. Peng, G.Y. Meng and B. Zhu, *J. Power Sources*, 104 (2002) 73.